

# Microscopically derived multi-component Ginzburg-Landau theories for $s + is$ superconducting state

Julien Garaud, Mihail Silaev, and Egor Babaev

Department of Theoretical Physics and Center for Quantum Materials,  
KTH-Royal Institute of Technology, Stockholm, SE-10691 Sweden

(Dated: September 10, 2022)

Starting with the generic Ginzburg-Landau expansion from a microscopic  $N$ -band model, we focus on the case of a 3-band model which was suggested to be relevant to describe some iron based superconductors. This can lead to the so-called  $s + is$  superconducting state that breaks time-reversal symmetry due to competition between different pairing channels. Of particular interest in that context, is the case of an interband dominated pairing with repulsion between different bands. For that case we consider in detail the relevant reduced two-component Ginzburg-Landau theory. We provide detailed analysis of the ground state, length-scales and topological properties of that model. *Prepared for the proceedings of Vortex IX conference in Rhodes September 2015*

## I. INTRODUCTION

In many superconductors, the pairing of electrons is supposed to take place in several sheets of a Fermi surface which is formed by the overlapping electronic bands. To name a few, this is for example the case of  $\text{MgB}_2$  [1],  $\text{Sr}_2\text{RuO}_4$  [2, 3] or in more recently discovered iron-based superconductors [4–6]. Properties of superconductors in multiband systems can be qualitatively different from their simplest single-band  $s$ -wave counterparts. Of particular interest are the states that break additional symmetries. Such states can appear if the superconducting gap functions phase differences between the bands differ from 0 or  $\pi$  [7–18]. Indeed in addition to the breakdown of the usual  $U(1)$  gauge symmetry, such superconducting states are characterized by an additional broken (discrete) time-reversal symmetry (BTRS). Spontaneous breakdown of time-reversal symmetry has various interesting physical consequences, many of which are currently being explored. Iron-based superconductors [3] are among the most promising candidates for the observation of time-reversal symmetry breaking state that originates in the multiband character of superconductivity and several competing pairing channels.

Experimental data suggest that in the hole-doped 122 compounds  $\text{Ba}_{1-x}\text{K}_x\text{Fe}_2\text{As}_2$ , the symmetry of superconducting state can change depending on the doping level  $x$ . A typical band structure of  $\text{Ba}_{1-x}\text{K}_x\text{Fe}_2\text{As}_2$  consists of two hole pockets at the  $\Gamma$  point and two electron pockets at  $(0, \pi)$  and  $(\pi, 0)$ . At moderate doping level  $x \sim 0.4$  various measurements, including ARPES [19–21], thermal conductivity [22] and neutron scattering experiments [23], are consistent with the hypothesis of an  $s_{\pm}$  state where the superconducting gap changes sign between electron and hole pockets. On the other hand, the symmetry of superconducting state at heavy doping  $x \rightarrow 1$  is not so clear regarding the question whether the  $d$  channel dominates or if the gap retains  $s_{\pm}$ -symmetry changing sign between the inner hole bands at the  $\Gamma$  point [24, 25]. Indeed, there are evidences that  $d$ -wave pairing channel dominates [26–29] while other ARPES data were

interpreted in favour of an  $s$ -wave symmetry [30, 31]. In both situations this implies the possible existence of an intermediate complex state that “compromises” between the behaviours at moderate and high doping. Depending on whether  $d$  or  $s$  channel dominates at heavy doping such complex state is named  $s + is$  or  $s + id$ .

The  $s + id$  state breaks  $C_4$  crystalline symmetry and is thus anisotropic, while the  $s + is$  state is qualitatively different as the  $C_4$  symmetry is preserved [17]. Note that the  $s + id$  superconducting state is also qualitatively different from the (time-reversal preserving)  $s + d$  states that attracted interest in the context of high-temperature cuprate superconductors (see e.g. [32–34]). It also contrasts with  $d + id$  state, which can appear in the presence of an external magnetic field, and that violates both parity and time-reversal symmetries [7]. While it is an interesting scenario, possibly relevant for pnictides, we will not further consider the properties of  $s + id$  state and focus on a detailed analysis of  $s + is$  superconducting state. This state is indeed of particular theoretical interest, being the simplest BTRS extension of the most abundant  $s$ -wave state. Also, it is expected to arise from various microscopic physics [10, 17, 35–38]. The  $s + is$  state could as well be fabricated on demand on the interfaces of superconducting bilayers [13].

To this day, no experimental proof of  $s + is$  nor  $s + id$  BTRS states have been reported. Indeed this requires probing the relative phases between components of the order parameter in different bands, which is a challenging task. For example the  $s + is$  state does not break the point group symmetries and is therefore not associated with intrinsic angular momentum of Cooper pairs. Consequently it cannot produce local magnetic field and thus is *a priori* invisible for conventional methods like muon spin relaxation and polar Kerr effect measurements that were for example used to probe time-reversal breaking  $p + ip$  superconducting state in e.g.  $\text{Sr}_2\text{RuO}_4$  compound [39]. Several proposals have been recently voiced, each with various limitations, for indirect observation of BTRS signature in pnictides. These for example include the investigation of the spectrum of the collective modes which includes massless [14] and mixed phase-density

[15, 17, 40, 41] excitations. Also, it was proposed to consider the properties of exotic topological excitations such as skyrmions and domain walls [42–44], unconventional mechanism of vortex viscosity [45], formation of vortex clusters [15], exotic reentrant and precursor phases induced by fluctuations [46–49]. Spontaneous currents were predicted to exist near non-magnetic impurities in anisotropic superconducting  $s+id$  states [8, 18] or in samples subjected to strain [18]. The latter proposal actually involves symmetry change of  $s+is$  states and relies on the presence of disorder which can typically have uncontrollable distribution. It was also recently pointed out that time-reversal symmetry breaking  $s+is$  state features an unconventional contribution to the thermoelectric effect [50]. Related to this an experimental set-up, based on a local heating was recently proposed [51]. The key idea being that local heating induces local variation of relative phases which further yield electromagnetic response that are directly observable.

The paper is organized as follows: in section II we start by deriving the GL expansion for a generic  $N$ -band model. Then we focus on the minimal three-band microscopic model suggested to describe hole-doped 122 compounds with three superconducting gaps. There we consistently derive the two-component Ginzburg-Landau equations that are relevant for interband dominated pairing. Next, section III is devoted to the analysis of the ground-state phases of the Ginzburg-Landau model. Then in section IV we introduce a reparametrization of the model that allows further investigation of the perturbative spectrum. This allows for example to derive the relevant length scales and the second critical field. Finally, section V is devoted to the analysis of the topological properties of the theory, together with the possible topological excitations.

## II. MICROSCOPIC MODEL AND DERIVATION OF THE MULTI-COMPONENT GINZBURG-LANDAU EXPANSION

We consider superconducting coupling which can result on BTRS state. A typical band structure of iron pnictides consists of two hole pockets at the  $\Gamma$  point and two electron pockets at  $(0, \pi)$  and  $(\pi, 0)$ . This structure is sketched on Fig. 1, where the dominating pairing channels are the interband repulsion between electron and hole bands, as well as between two hole pockets at  $\Gamma$ . Note that there, the order parameter is the same in both electron pockets so that the crystalline  $C_4$  symmetry is not broken and thus corresponds to an  $s$  state. This contrasts with an alternative scenario which was proposed in pnictides, the strongest interactions are the repulsions between hole and electron bands and between two electron pockets. Such interaction favours order parameter sign change between electron pockets resulting in a  $C_4$  symmetry breaking  $d$ -wave state. Such a scenario also allows BTRS phase in the form of an  $s+id$  superconduct-

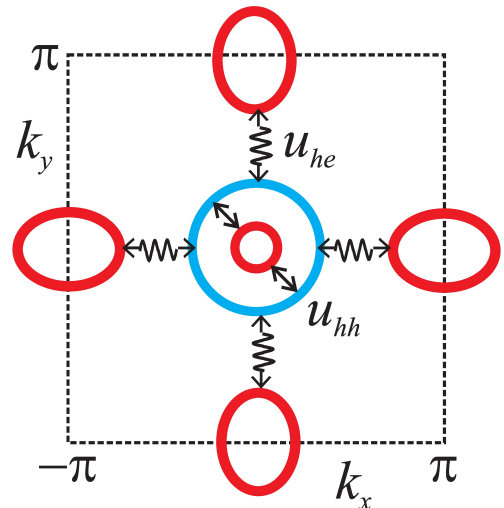


Figure 1. (Color online) – Schematic view of the band structure in hole-doped iron pnictide compound  $\text{Ba}_{1-x}\text{K}_x\text{Fe}_2\text{As}_2$ . It consists of two hole pockets at  $\Gamma$  shown by circles and two electron pockets at  $(0, \pi)$  and  $(\pi, 0)$  shown by ellipses. As discussed in the text, the  $s+is$  state is favoured by superconducting coupling dominated by the interband repulsion between electron and hole Fermi surfaces  $u_{he}$ , as well as between the two hole pockets  $u_{hh}$ .

ing state. As symmetrywise it is qualitatively different from the  $s+is$  state, the case of an  $s+id$  superconducting state is not discussed here.

### A. Generic $N$ -component expansion

To derive a Ginzburg-Landau expansion that can be used for example in numerical simulations, we consider the microscopic model of clean superconductor with, in general,  $N$  overlapping bands at the Fermi level. Within the quasiclassical approximation, the band parameters that characterize the different cylindrical sheets of the Fermi surface are the Fermi velocities  $\mathbf{v}_F^{(j)}$  and the partial densities of states (DOS)  $\nu_j$ , where the label  $j = 1, \dots, N$  denotes the band index. The particular example of a three-band model believed to be relevant in 122 compounds and which is considered in details below, is schematically shown in Fig. 1. The Eilenberger equations for quasiclassical propagators read as

$$\hbar \mathbf{v}_F^{(j)} \boldsymbol{\Pi} f_j + 2\omega_n f_j - 2\Delta_j g_j = 0, \quad (1a)$$

$$\hbar \mathbf{v}_F^{(j)} \boldsymbol{\Pi}^* f_j^+ - 2\omega_n f_j^+ + 2\Delta_j^* g_j = 0, \quad (1b)$$

where  $\boldsymbol{\Pi} = \nabla - 2\pi i \mathbf{A}/\Phi_0$ ,  $\mathbf{A}$  is the vector potential, and  $\Phi_0$  the flux quantum. The quasiclassical Green's functions in each band obey the normalization condition  $g_j^2 + f_j f_j^+ = 1$ . Finally, the self-consistency equation for

the gaps and the electric current are

$$\Delta_i(\mathbf{p}, \mathbf{r}) = 2\pi T \sum_{n, \mathbf{p}', j} \lambda_{ij}(\mathbf{p}, \mathbf{p}') f_j(\mathbf{p}, \mathbf{r}, \omega_n), \quad (2)$$

$$\mathbf{j}(\mathbf{r}) = 2\pi e T \sum_{n, \mathbf{p}, j} \nu_j \mathbf{v}_F^{(j)} \text{Im } g_j(\mathbf{p}, \mathbf{r}, \omega_n). \quad (3)$$

Here  $g_j = \text{sign}(\omega_n) \sqrt{1 - f_j f_j^+}$  and  $\nu_j$  is the density of states, the parameters  $\mathbf{p}$  run over the corresponding Fermi surfaces and  $\lambda_{ij}$  are the components of the coupling potential matrix. For simplicity we further consider isotropic pairing states so that on each of the Fermi surfaces  $\lambda_{ij}(\mathbf{p}, \mathbf{p}') = \text{const}$ . However, in electron pockets we keep the anisotropy of Fermi velocities in Eqs.(1). The anisotropy of hole bands on the other hand can be neglected, which is a well-justified assumption [52].

The derivation of the GL functional from the microscopic equations formally follows the standard scheme. That is by expressing the solutions of Eilenberger equations in the form of the expansion by powers of the gap functions amplitudes  $\Delta_j$  and their gradients. We stress that this multiband expansion relies on the existence of above-mentioned multiple small parameters. This is in contrast to the simplest single-band Ginzburg-Landau expansion that is justified by a single small parameter  $(1 - T/T_c)$ . For a multi-band GL expansion, using a single small parameter is in general incorrect or irrelevant due to the existence of multiple broken symmetries. Also, even in the case of a multiband system breaking a single symmetry, an expansion that is obtain relying on a single small parameter in certain cases has vanishingly small applicability range [53]. For earlier works on microscopic two-band GL expansions see [54–57] and the analysis is straightforwardly generalized to similar  $s$ -wave  $N$ -component cases. First, the solutions of Eqs.(1) are found in the form of the expansion by powers of the gap functions amplitudes  $\Delta_j$  and their gradients:

$$f_j(\mathbf{p}, \mathbf{r}, \omega_n) = \frac{\Delta_j}{\omega_n} - \frac{|\Delta_j|^2 \Delta_j}{2\omega_n^3} - \frac{\hbar(\mathbf{v}_F^{(j)} \mathbf{\Pi}) \Delta_j}{2\omega_n^2} + \frac{\hbar^2(\mathbf{v}_F^{(j)} \mathbf{\Pi})(\mathbf{v}_F^{(j)} \mathbf{\Pi}) \Delta_j}{4\omega_n^3} \quad (4)$$

and  $f_j^+(\mathbf{p}, \mathbf{r}, \omega_n) = f_j^*(-\mathbf{p}, \mathbf{r}, \omega_n)$ . Then, the summation over Matsubara frequencies gives

$$2\pi T \sum_{n=0}^{N_d} \omega_n^{-1} = G_0 + \tau, \quad \text{with } \tau = (1 - T/T_c). \quad (5)$$

The gaps are normalized by  $T_c/\sqrt{\rho}$  (where  $\rho = \sum_n \pi T_c^3 \omega_n^{-3} \approx 0.1$ ) and, substitution of (4) into the self-consistency Eqs.(2) determines the system of GL equations

$$[(G_0 + \tau - \hat{\Lambda}^{-1}) \mathbf{\Delta}]_j = -K_{ab}^{(j)} \Pi_a \Pi_b \Delta_j + |\Delta_j|^2 \Delta_j, \quad (6)$$

where  $\mathbf{\Delta} = (\Delta_1 \dots \Delta_N)^T$ . The anisotropy tensor is  $K_{ab}^{(j)} = \hbar^2 \rho \langle v_{Fa}^{(j)} v_{Fb}^{(j)} \rangle / 2T_c^2$  where the average is taken over the  $j$ -th Fermi surface and  $a, b$  stand for the  $x, y$  coordinates.

The current reads as

$$\mathbf{J}(\mathbf{r}) = \frac{4e}{\hbar} \frac{T_c^2}{\rho} \sum_{i=1}^N \nu_i \text{Im } \Delta_i^* \hat{K}_i \mathbf{\Pi} \Delta_i. \quad (7)$$

The critical temperature is determined by the equation  $G_0 = \min_n(\lambda_n^{-1})$ , where  $\lambda_n^{-1}$  are the positive eigenvalues of the inverse coupling matrix  $\hat{\Lambda}^{-1}$ . Provided that all the eigenvalues are positive, the number of components of the order parameter coincide with the number of bands  $N$ . In this case, the system of Ginzburg-Landau equations for the general  $N$ -component system can be written as follows

$$-K_{ab}^{(i)} \Pi_a \Pi_b \Delta_i + \alpha_i \Delta_i + \eta_{ij} \Delta_j + \beta_i |\Delta_i|^2 \Delta_i = 0, \quad (8)$$

where

$$\alpha_i = (\hat{\Lambda}_{ij}^{-1} - G_0 - \tau) \delta_{ij}, \quad (9a)$$

$$\eta_{ij} = (1 - \delta_{ij}) \hat{\Lambda}_{ij}^{-1} \quad \text{and} \quad \beta_i = 1. \quad (9b)$$

Various choices of microscopic coupling parameters can result in qualitatively different structures of the Ginzburg-Landau field theory.

## B. Ginzburg-Landau models for the $s + is$ state

Our main interest here is the time-reversal symmetry breaking  $s + is$  states in three-band systems. Let us consider first the simplest case of an intraband dominated pairing which can be described by a three-component GL theory in the vicinity of  $T_c$ . This regime is described by the following coupling matrix

$$\hat{\Lambda} = \begin{pmatrix} \lambda & -\eta_h & -\eta_e \\ -\eta_h & \lambda & -\eta_e \\ -\eta_e & -\eta_e & \lambda \end{pmatrix}, \quad (10)$$

where  $\eta_e, \eta_h \ll \lambda$ . The critical temperature is determined by the equation  $G_0 = \min(\lambda_1^{-1}, \lambda_2^{-1}, \lambda_3^{-1})$ , where  $\lambda_{1,2}^{-1} = (2\lambda - \eta_h \pm \sqrt{8\eta_e^2 + \eta_h^2}) / [2(\lambda^2 - \lambda\eta_h - 2\eta_e^2)]$  and  $\lambda_3^{-1} = 1/(\lambda + \eta_h)$  are the positive eigenvalues of the inverse coupling matrix

$$\hat{\Lambda}^{-1} = X \begin{pmatrix} \lambda^2 - \eta_e^2 & \eta_e^2 + \lambda\eta_h & \eta_e(\lambda + \eta_h) \\ \eta_e^2 + \lambda\eta_h & \lambda^2 - \eta_e^2 & \eta_e(\lambda + \eta_h) \\ \eta_e(\lambda + \eta_h) & \eta_e(\lambda + \eta_h) & \lambda^2 - \eta_h^2 \end{pmatrix}, \quad (11)$$

where  $X = 1/[(\lambda^2 - \lambda\eta_h - 2\eta_e^2)(\lambda + \eta_h)]$ . Since we assume that  $\eta_{e,h} > 0$  and  $\eta_{e,h} \ll \lambda$ , the critical temperature is given by the smallest eigenvalue  $G_0 = 1/(\lambda + \eta_h)$  so that

$$G_0 - \hat{\Lambda}^{-1} = - \begin{pmatrix} a_1 & a_1 & a_2 \\ a_1 & a_1 & a_2 \\ a_2 & a_2 & a_3 \end{pmatrix}, \quad (12)$$

where

$$a_1 = (\eta_e^2 + \lambda\eta_h)/X \quad (13a)$$

$$a_2 = \eta_e(\lambda + \eta_h)/X \quad (13b)$$

$$a_3 = (2\eta_e^2 - \eta_h^2 + \lambda\eta_h)/X. \quad (13c)$$

The free energy functional whose variations give the three-component Ginzburg-Landau equations reads as

$$\mathcal{F} = \frac{B^2}{2} + \sum_{j=1}^3 \left\{ \frac{k_j}{2} |\mathbf{\Pi} \Delta_j|^2 + \alpha_j |\Delta_j|^2 + \frac{\beta_j}{2} |\Delta_j|^4 \right\} + \sum_{j=1}^3 \sum_{k=j+1}^3 \eta_{jk} \left\{ \Delta_j^* \Delta_k + \Delta_k^* \Delta_j \right\}, \quad (14)$$

where  $\beta_k = 1$ ,  $\eta_{12} = a_1$ ,  $\eta_{13} = \eta_{23} = a_2$ ,  $\alpha_k = \alpha_k^0(T/T_k - 1)$ ,  $\alpha_k^0 = 1 - a_k$ ,  $T_k = T_c(1 - a_k)$ . Here we assumed that bands are isotropic and put  $K_{xx}^{(j)} = K_{yy}^{(j)} = k_j \xi_0^2/2$  and introduce the dimensional units normalizing lengths by  $\xi_0 = \hbar \bar{v}_F / T_c$  (where  $\bar{v}_F$  is the average value of Fermi velocity), magnetic field by  $B_0 = T_c \sqrt{8\pi\nu/\rho}$ , current density  $j_0 = cB_0/(4\pi\xi_0)$  and free energy density  $F_0 = B_0^2/8\pi$ . Here  $\nu$  is the DOS which is assumed to be the same in all superconducting bands. In such units the electric charge is replaced by an effective coupling constant  $\tilde{e} = 2\pi B_0 \xi_0^2 / \Phi_0$  so that  $\mathbf{\Pi} = \nabla + i\tilde{e}\mathbf{A}$ . Below we omit the tilde for brevity.

In the following, we consider another choice of the coupling matrix  $\hat{\Lambda}$ , suggested to be relevant for iron-based superconductors [17, 37, 41]. It corresponds to the case of an interband dominated pairing with repulsion, parametrized as

$$\hat{\Lambda} = - \begin{pmatrix} 0 & \eta & \lambda \\ \eta & 0 & \lambda \\ \lambda & \lambda & 0 \end{pmatrix}. \quad (15)$$

Here  $\Delta_{1,2}$  correspond to the gaps at hole Fermi surfaces and  $\Delta_3$  is the gap at electron pockets so that the coefficients  $\eta = u_{hh}$  and  $\lambda = u_{eh}$  are respectively the hole-hole and electron-hole interactions. Neglecting the r.h.s. in (6) we get the linear equation which determines the critical temperature  $G_0 = \min(G_1, G_2)$ , where  $G_1 = 1/\eta$  and  $G_2 = (\eta + \sqrt{\eta^2 + 8\lambda^2})/4\lambda^2$  are the positive eigenvalues of the matrix

$$\hat{\Lambda}^{-1} = \frac{1}{2\lambda^2\eta} \begin{pmatrix} \lambda^2 & -\lambda^2 & -\lambda\eta \\ -\lambda^2 & \lambda^2 & -\lambda\eta \\ -\lambda\eta & -\lambda\eta & \eta^2 \end{pmatrix}. \quad (16)$$

The coupling matrix  $\hat{\Lambda}^{-1}$  has only two positive eigenvalues  $G_{1,2}$  whose eigenvectors are  $\mathbf{\Delta}_1 = (-1, 1, 0)^T$  and  $\mathbf{\Delta}_2 = (x, x, 1)^T$  with  $x = (\eta - \sqrt{\eta^2 + 8\lambda^2})/4\lambda$ . Since only the fields corresponding to the positive eigenvalues can nucleate, the GL theory (6) has to be reduced to a two-component one. To implement this reduction the general order parameter is expressed in terms of the superposition

$$\mathbf{\Delta} = \psi_1 \mathbf{\Delta}_1 + \psi_2 \mathbf{\Delta}_2,$$

$$\text{and } (\Delta_1, \Delta_2, \Delta_3) = (x\psi_2 - \psi_1, x\psi_2 + \psi_1, \psi_2). \quad (17)$$

There,  $\psi_1$  and  $\psi_2$  are the order parameter of  $s_{\pm}$  pairing channels between two concentric hole surfaces and between hole and electron surfaces correspondingly.

Now, substituting the ansatz (17) into the system of Ginzburg-Landau equations (6) we obtain, after projection on the vectors  $\mathbf{\Delta}_{1,2}$ , the system of two GL equations

$$a_1 \psi_1 + b_{1j} |\psi_j|^2 \psi_1 + b_J \psi_1^* \psi_2^2 = \quad (18a)$$

$$(K_{aa}^{(1)} + K_{aa}^{(2)}) \Pi_a^2 \psi_1 + x(K_{aa}^{(2)} - K_{aa}^{(1)}) \Pi_a^2 \psi_2$$

$$a_2 \psi_2 + b_{2j} |\psi_j|^2 \psi_2 + b_J \psi_2^* \psi_1^2 = \quad (18b)$$

$$\left[ x^2 (K_{aa}^{(1)} + K_{aa}^{(2)}) + K_{aa}^{(3)} \right] \Pi_a^2 \psi_2 + x(K_{aa}^{(2)} - K_{aa}^{(1)}) \Pi_a^2 \psi_1.$$

The parameters of the left hand side of the Ginzburg-Landau equations (18) are expressed, in terms of the coefficients of the coupling matrix (15) as

$$a_j = -|\mathbf{\Delta}_j|^2 (G_0 - G_j + \tau), \quad (19a)$$

$$\text{with } |\mathbf{\Delta}_1|^2 = 2 \text{ and } |\mathbf{\Delta}_2|^2 = 2x^2 + 1 \quad (19b)$$

$$b_{11} = 2, \quad b_{22} = (2x^4 + 1) \text{ and } b_k := b_{kk} \quad (19c)$$

$$b_{12} = 4x^2, \quad b_J = 2x^2. \quad (19d)$$

As previously stated, the  $s + is$  state is symmetric under  $C_4$  transformations, which implies that  $K_{xx}^{(j)} = K_{yy}^{(j)} = K^{(j)}$ . The Ginzburg-Landau equations can thus be further simplified as follows

$$a_1 \psi_1 + b_{1j} |\psi_j|^2 \psi_1 + b_J \psi_1^* \psi_2^2 = \frac{k_{1j}}{2} \mathbf{\Pi}^2 \psi_j, \quad (20a)$$

$$a_2 \psi_2 + b_{2j} |\psi_j|^2 \psi_2 + b_J \psi_2^* \psi_1^2 = \frac{k_{2j}}{2} \mathbf{\Pi}^2 \psi_j, \quad (20b)$$

where the coefficients of the gradient terms read as

$$k_{11} := k_1 = 2\xi_0^{-2} [K^{(1)} + K^{(2)}] \quad (21a)$$

$$k_{22} := k_2 = 2\xi_0^{-2} [(K^{(1)} + K^{(2)})x^2 + K^{(3)}] \quad (21b)$$

$$k_{12} = 2\xi_0^{-2} x [K^{(2)} - K^{(1)}]. \quad (21c)$$

The total current (7), which can be expressed in terms of the partial currents  $\mathbf{J}^{(i)}$  of the different components of order parameters, reads as  $\mathbf{J} = \sum_i \mathbf{J}^{(i)}$ ; and the partial currents read as

$$\mathbf{J}^{(i)} = e \text{Im}(\psi_i^* [k_i \mathbf{\Pi} \psi_i + k_{12} \mathbf{\Pi} \psi_j]), \quad (22)$$

where  $j \neq i$ .

The two component free energy functional that corresponds to the Ginzburg-Landau equations (20), and whose variations with respect to  $\mathbf{A}$  give the supercurrent (22), reads as (in dimensionless units):

$$\mathcal{F} = \frac{B^2}{2} + \sum_{j=1}^2 \left\{ \frac{k_j}{2} |\mathbf{\Pi} \psi_j|^2 + a_j |\psi_j|^2 + \frac{b_j}{2} |\psi_j|^4 \right\} \quad (23a)$$

$$+ \frac{k_{12}}{2} \left( (\mathbf{\Pi} \psi_1)^* \mathbf{\Pi} \psi_2 + (\mathbf{\Pi} \psi_2)^* \mathbf{\Pi} \psi_1 \right) \quad (23b)$$

$$+ b_{12} |\psi_1|^2 |\psi_2|^2 + \frac{b_J}{2} (\psi_1^* \psi_2^2 + \text{c.c.}). \quad (23c)$$

Here, the complex fields  $\psi_j = |\psi_j|e^{i\theta_j}$  represent the components of the order parameter. These are electromagnetically coupled by the vector potential  $\mathbf{A}$  of the magnetic field  $\mathbf{B} = \nabla \times \mathbf{A}$ , through the gauge derivative  $\Pi \equiv \nabla + ie\mathbf{A}$  where the coupling constant  $e$  is used to parametrize the London penetration length. Note that for the energy to be positively defined, the coefficients of the kinetic terms should satisfy the relation  $k_1 k_2 - k_{12}^2 > 0$ . Also, for the free energy functional to be bounded from below, the coefficients of the terms that are fourth order in the condensates should satisfy the constraint  $b_1 b_2 - (b_{12} + b_J)^2 > 0$ . These conditions are of course satisfied by the microscopically calculated value (19) and (21).

### III. GROUND-STATE PROPERTIES OF THE TWO-COMPONENT GINZBURG-LANDAU MODEL

Depending on the relation between the parameters of the potential, qualitatively different superconducting phases can be identified. These are determined by the ground-state properties of the theory. Since the coefficients of the kinetic terms satisfy the relation  $k_1 k_2 - k_{12}^2 > 0$ , the ground state is homogeneous ( $\Pi\psi_k = 0$ ) and thus

it is determined only from the potential terms of (23) that reads as:

$$V = \sum_{j=1}^2 a_j |\psi_j|^2 + \frac{b_j}{2} |\psi_j|^4 + |\psi_1|^2 |\psi_2|^2 (b_{12} + b_J \cos \theta_{12}), \quad (24)$$

where  $\theta_{12} = \theta_2 - \theta_1$  is the relative phase between both condensates. Ground state is the state denoted by  $\psi_k = u_k e^{i\theta_k}$ , and where the vector potential is a pure gauge ( $\mathbf{A} = \nabla\chi$  for arbitrary  $\chi$ ) that can consistently chosen to be zero.  $\partial V / \partial u_j = 0$  and  $\partial V / \partial \theta_{12} = 0$ . The ground state  $[u_1, u_2, \theta_{12}]$ , being an extremum of that potential thus satisfies:

$$\begin{cases} 2(a_1 + b_1 u_1^2 + (b_{12} + b_J \cos 2\theta_{12})u_2^2) u_1 = 0 & (25a) \\ 2(a_2 + b_2 u_2^2 + (b_{12} + b_J \cos 2\theta_{12})u_1^2) u_2 = 0 & (25b) \\ -2b_J u_1^2 u_2^2 \sin 2\theta_{12} = 0. & (25c) \end{cases}$$

Besides being an extremum according to the condition (25), the ground state should also be a minimum. That is, the eigenvalues of the Hessian matrix must be positive. The Hessian matrix reads as

$$\mathcal{H} = 2 \begin{pmatrix} a_1 + 3b_1 u_1^2 + (b_{12} + b_J \cos 2\theta_{12})u_2^2 & 2(b_{12} + b_J \cos 2\theta_{12})u_1 u_2 & -2b_J u_1 u_2^2 \sin 2\theta_{12} \\ 2(b_{12} + b_J \cos 2\theta_{12})u_1 u_2 & a_2 + 3b_2 u_2^2 + (b_{12} + b_J \cos 2\theta_{12})u_1^2 & -2b_J u_1^2 u_2 \sin 2\theta_{12} \\ -2b_J u_1 u_2^2 \sin 2\theta_{12} & -2b_J u_1^2 u_2 \sin 2\theta_{12} & -2b_J u_1^2 u_2^2 \cos 2\theta_{12} \end{pmatrix} \quad (26)$$

Besides the normal state  $[u_1, u_2, \theta_{12}] = [0, 0, \theta_{12}]$ , the model (23) features various ground state phases, depending on the parameters of the theory.

#### A. Normal state

By definition, the normal state is the state with no superconducting condensate:  $[u_1, u_2, \theta_{12}] = [0, 0, \theta_{12}]$ . The Hessian matrix (26) for that state

$$\mathcal{H} = 2 \begin{pmatrix} a_1 & 0 & 0 \\ 0 & a_2 & 0 \\ 0 & 0 & 0 \end{pmatrix}, \quad (27)$$

gives the minimal stability condition  $a_1, a_2 > 0$  of the normal state.

#### B. Phase separated phase

Here, the term *phase separated phase* relates to the case where only *one* of Ginzburg-Landau component assumes a non-zero ground state density, while the second

is completely suppressed. That is either  $[u_1, u_2, \theta_{12}] = [\sqrt{-a_1/b_1}, 0, \theta_{12}]$  or  $[0, \sqrt{-a_2/b_2}, \theta_{12}]$ . For example, if only the first component has a non-zero ground-state density, the Hessian reads as

$$\mathcal{H} = 2 \begin{pmatrix} -2a_1 & 0 & 0 \\ 0 & a_2 + (b_{12} + b_J \cos 2\theta_{12})u_1^2 & 0 \\ 0 & 0 & 0 \end{pmatrix}. \quad (28)$$

Note that the case where only the second component is nonzero can easily be obtained by permuting “1,2” indices.

These ground states correspond, in the microscopic 3-band model, to two physically different states. The case  $u_1 \neq 0$  and  $u_2 = 0$  gives the sign changing gap ( $s_{\pm}$ ) with  $\Delta_3 = 0$ . On the other hand, the case  $u_2 \neq 0$  and  $u_1 = 0$  gives the  $s_{++}$  state.

#### C. Coexisting phase

This is the phase where both  $u_1, u_2 \neq 0$ , that we are principally interested in, in this paper. Observe that Eq. (25c) specifies the ground state relative phase be-



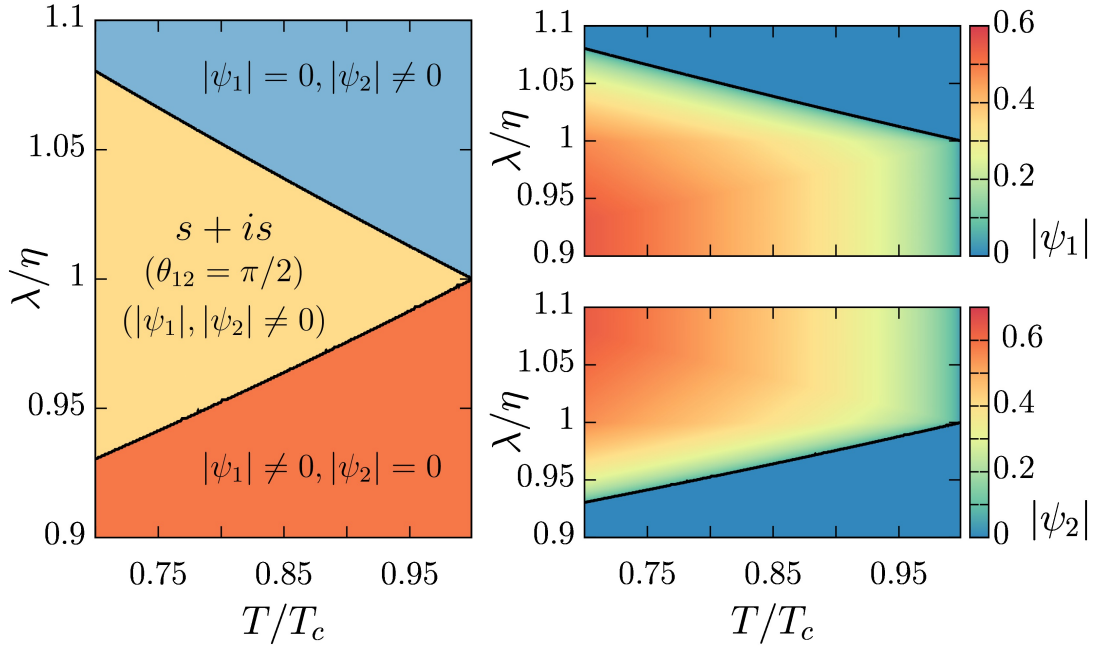


Figure 2. (Color online) – Left panel displays the different phases. In the  $s + is$  state, the relative phase is  $\pi/2$ . The panels on the right show the ground state densities  $|\psi_1|$  and  $|\psi_2|$ . All parameters of the GL functional were calculated using the relations (19) where we used  $\eta = 0.5$ .

tween both condensates to be an integer multiple of  $\pi/2$ , when both condensates have nonzero density  $u_1, u_2 \neq 0$ . Introducing for convenience  $d = b_{12} + b_J \cos n\pi$ , and since the  $b_1 b_2 - d^2 > 0$ , for the free energy functional to be bounded from below, the ground state is

$$[u_1, u_2, \theta_{12}] = \left[ \sqrt{\frac{a_2 d - a_1 b_2}{b_1 b_2 - d^2}}, \sqrt{\frac{a_1 d - a_2 b_1}{b_1 b_2 - d^2}}, \frac{n\pi}{2} \right] \quad (29)$$

and the Hessian matrix becomes

$$\mathcal{H} = 4 \begin{pmatrix} b_1 u_1^2 & du_1 u_2 & 0 \\ du_1 u_2 & b_2 u_2^2 & 0 \\ 0 & 0 & -2b_J u_1^2 u_2^2 \cos n\pi \end{pmatrix}. \quad (30)$$

Obviously, if  $b_J < 0$  (resp.  $b_J > 0$ ) then the stable state has  $n$  which is an even (resp. odd) integer and thus the ground state relative phase is  $\pm\pi/2$  (resp.  $0, \pi$ ) and thus  $d = b_{12} + |b_J|$ . The condition for the stability of the coexisting phase thus boils down to having positive eigenvalues for the reduced Hessian

$$\mathcal{H} = 4 \begin{pmatrix} b_1 u_1^2 & (b_{12} + |b_J|) u_1 u_2 \\ (b_{12} + |b_J|) u_1 u_2 & b_2 u_2^2 \end{pmatrix}. \quad (31)$$

#### D. Ginzburg-Landau phase diagram of the $s + is$ state

Here we are principally interested in the  $s + is$  state. That is in the phase where both condensates coexist and

the time-reversal symmetry is spontaneously broken (i.e. when  $\theta = \pm\pi/2$ ). The ground state thus reads as

$$[u_1, u_2, \theta_{12}] = \left[ \sqrt{\frac{a_2 d - a_1 b_2}{b_1 b_2 - d^2}}, \sqrt{\frac{a_1 d - a_2 b_1}{b_1 b_2 - d^2}}, \pm \frac{\pi}{2} \right] \quad (32)$$

in the region of the parameter space defined by

$$b_1 b_2 - (b_{12} + b_J)^2 > 0 \quad (33)$$

$$a_2 d - a_1 b_2 > 0 \quad (34)$$

$$a_1 d - a_2 b_1 > 0. \quad (35)$$

The physical system we are interested in here, is the microscopic three-band model (15) with interband dominated pairing with repulsion, that is believed to be relevant for some pnictides. There, the parameters of the Ginzburg-Landau model (23) actually depend on few microscopic parameters of the coupling matrix and the reduced temperature, as shown on (19). Fig. 2 shows the ground state phase diagram of the Ginzburg-Landau model as a function of the reduced temperature and the ratio of electron-hole and hole-hole interactions.

#### IV. ELIMINATION OF MIXED GRADIENTS AND SEPARATION OF CHARGED AND NEUTRAL MODES

The current basis for the superconducting degrees of freedom is quite convenient, as it allows to easily characterize the ground state and its stability properties. On

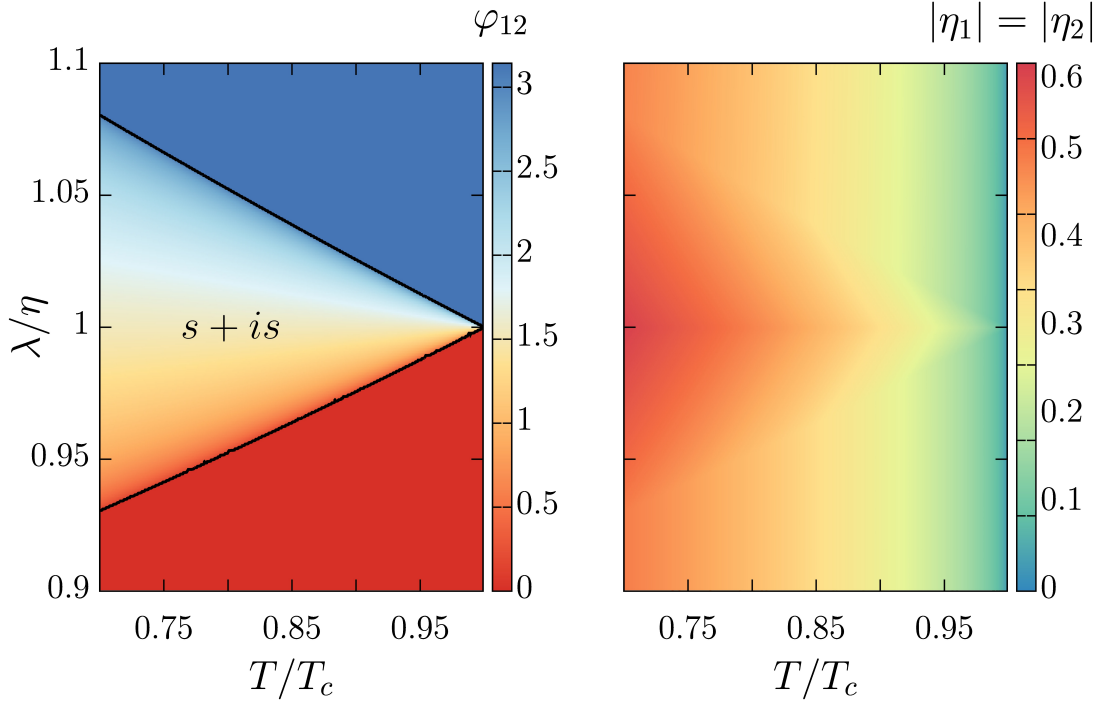


Figure 3. (Color online) – Ground state phase diagram in the  $\eta$  parametrization where there are no mixed gradients. Left panel displays the different phases. In the  $s + is$  state, the relative phase is different from 0,  $\pi$ . The right panel show the ground state densities  $|\eta_1| = |\eta_2|$ . This is for the same values of the microscopic parameters as in Fig. 2 and for the value of the coefficients of the kinetic terms  $K^{(1)} = 0.5$ ,  $K^{(2)} = 0.05$  and  $K^{(3)} = 0.25$ .

the other hand, it is quite complicated to deal with the kinetic terms. This is why it is worth rewriting the model using a linear combination of the components of the order parameter that diagonalize the the kinetic terms:

$$\eta_1 = \sqrt{k_1}\psi_1 + \sqrt{k_2}\psi_2, \quad \eta_2 = \sqrt{k_1}\psi_1 - \sqrt{k_2}\psi_2. \quad (36)$$

Within this new basis, the kinetic term has a much simpler form. The potential, on the other hand becomes much more complicated and at first glance it is not possible to find the ground state analytically. However, since it is known in the old field basis, it is actually simple to derive the analytic solution. It is also a convenient basis to deal with the determination of the physical length scales as well as describing various unusual properties.

In the new field basis, the free energy reads as

$$\mathcal{F} = \frac{\mathbf{B}^2}{2} + \sum_{a=1}^2 \frac{\kappa_a}{2} |\Pi_j \eta_a|^2 + \alpha |\eta_a|^2 + \frac{\beta}{2} |\eta_a|^4 \quad (37a)$$

$$+ (\nu + \omega (|\eta_1|^2 + |\eta_2|^2)) |\eta_1| |\eta_2| \cos \varphi_{12} \quad (37b)$$

$$+ (\gamma + \delta \cos 2\varphi_{12}) |\eta_1|^2 |\eta_2|^2, \quad (37c)$$

with  $\eta_a = |\eta_a|e^{i\varphi_a}$ ,  $\varphi_{12} = \varphi_2 - \varphi_1$  and the coefficients for the kinetic term are now

$$\kappa_1 = \frac{\sqrt{k_1 k_2} + k_{12}}{2\sqrt{k_1 k_2}} \quad \text{and} \quad \kappa_2 = \frac{\sqrt{k_1 k_2} - k_{12}}{2\sqrt{k_1 k_2}}. \quad (38)$$

The coefficients of the potential read as

$$\begin{aligned} \alpha &= \frac{a_1 k_2 + a_2 k_1}{4k_1 k_2} \\ \nu &= \frac{a_1 k_2 - a_2 k_1}{2k_1 k_2} \\ \beta &= \frac{b_1 k_2^2 + b_2 k_1^2 + 2k_1 k_2 (b_{12} + b_J)}{16k_1^2 k_2^2} \\ \omega &= \frac{b_1 k_2^2 - b_2 k_1^2}{8k_1^2 k_2^2} \\ \gamma &= \frac{b_1 k_2^2 + b_2 k_1^2 - 2k_1 k_2 b_J}{8k_1^2 k_2^2} \\ \delta &= \frac{b_1 k_2^2 + b_2 k_1^2 + 2k_1 k_2 (b_J - b_{12})}{16k_1^2 k_2^2}. \end{aligned} \quad (39)$$

In the new variables, the Ginzburg-Landau equations have no mixed gradients and read as

$$\Pi^2 \eta_i = 2 \frac{\partial V}{\partial \eta_i^*}, \quad (40)$$

while variation of the free energy (37) with respect to the vector potential  $\mathbf{A}$ , determines Ampère's equation  $\nabla \times \mathbf{B} + \mathbf{J} = 0$ . The total current is the superposition of the partial currents ( $\mathbf{J} = \sum_k \mathbf{J}^{(k)}$ ) that reads as

$$\mathbf{J}^{(i)} = e\kappa_i \text{Im}(\eta_i^* \Pi \eta_i). \quad (41)$$

This reparametrization simplifies drastically the Ginzburg-Landau equations as there is no more coupling of the components through mixed gradients. However, this comes with the price of more complicated potential terms. This is actually a minor problem, since the ground state within the new basis, can easily be determined from the one in the old basis according to the formulas

$$\begin{aligned} |\eta_1|^2 &= k_1|\psi_1|^2 + k_2|\psi_2|^2 + 2\sqrt{k_1k_2}|\psi_1||\psi_2|\cos\theta_{12}, \\ |\eta_2|^2 &= k_1|\psi_1|^2 + k_2|\psi_2|^2 - 2\sqrt{k_1k_2}|\psi_1||\psi_2|\cos\theta_{12}, \\ \varphi_{12} &= \tan^{-1}\left(\frac{-2\sqrt{k_1k_2}|\psi_1||\psi_2|\sin\theta_{12}}{k_1|\psi_1|^2 - k_2|\psi_2|^2}\right). \end{aligned} \quad (42)$$

Fig. 3 shows the ground state phase diagram expressed in the new parametrization (37). Note that the ground state diagram Fig. 2 do not depend on the values the components of the (microscopic) anisotropy tensor. Since the reparametrization (36) explicitly depends on the parameters of the kinetic terms, the diagram Fig. 3 also depends on them. However this dependence can be only quantitative, since obviously the phase diagram cannot depend on any particular choice of parametrization.

### A. Separation of charged and neutral modes

To understand the role of the fundamental excitations, as well as the fundamental length scales of the Ginzburg-Landau free energy (37), it can be rewritten in terms of *charged* and *neutral* modes by expanding the kinetic term in (37a) and using (41):

$$\begin{aligned} \mathcal{F} &= \frac{1}{2}(\nabla \times \mathbf{A})^2 + \frac{\mathbf{J}^2}{2e^2\varrho^2} + \sum_a \frac{\kappa_a}{2}(\nabla|\eta_a|)^2 \\ &+ \frac{\kappa_1\kappa_2|\eta_1|^2|\eta_2|^2}{2\varrho^2}(\nabla\varphi_{12})^2 + V(|\eta_1|, |\eta_2|, \varphi_{12}). \end{aligned} \quad (43)$$

Here  $\varphi_{12} \equiv \varphi_2 - \varphi_1$  stands for the relative phase between the condensates. For this rewriting, we used the supercurrent defined from the Ampère's equation  $\nabla \times \mathbf{B} + \mathbf{J} = 0$ , that reads

$$\begin{aligned} \mathbf{J}/e &= e\varrho^2\mathbf{A} + \sum_a \kappa_a|\eta_a|^2\nabla\varphi_a, \\ \text{with } \varrho^2 &= \sum_a \kappa_a|\eta_a|^2. \end{aligned} \quad (44)$$

As discussed below, this formulation allows better interpretation of the small perturbations and their length scales, as well as better understanding of the elementary topological excitations of the theory.

### B. Coherence lengths and perturbation operator

The length scales characterising matter field are coherence lengths. These are, by definition, inverse masses of the infinitesimal perturbations around the ground state. More precisely, we consider small perturbations by linearising the theory around the ground-state. The eigenspectrum of the obtained (linear) differential operator determines the masses of the elementary excitations and thus their corresponding length-scales. The perturbation theory is constructed as follows. The fields are expanded in series of a small parameter  $\epsilon$ :  $\eta_a = \sum_i \epsilon^i \eta_a^{(i)}$  and collected order by order in the functional. The zeroth order is the original functional, while the first order is identically zero provided the leading order in the series expansion satisfies the equations of motion. Physically relevant correction thus appear at the order  $\epsilon^2$  of the expanded Ginzburg-Landau functional. The length-scale analysis is done by applying the previously discussed perturbative theory to the case where the leading order is the ground-state. As the ground state is homogeneous, the perturbation operator will drastically simplify. We choose the following perturbative expansion around the ground state

$$\eta_a = u_a + \frac{\epsilon f_a}{\sqrt{\kappa_a}}, \quad \varphi_{12} = \bar{\varphi} + \epsilon \sqrt{\frac{\kappa_1 u_1^2 + \kappa_2 u_2^2}{\kappa_1 \kappa_2 u_1^2 u_2^2}} \phi. \quad (45)$$

where  $u_a$  and  $\bar{\varphi}$  denote the ground state and  $f_a$ ,  $\Upsilon$ , the perturbations. Collecting the perturbations in  $\Upsilon = (f_1, f_2, \phi)^T$  the term which is second order in  $\epsilon$  in the Ginzburg-Landau functional reads as:

$$\frac{1}{2}\Upsilon^T (\nabla^2 + \mathcal{M}^2) \Upsilon, \quad (46)$$

where the entries of the (squared) mass matrix are:



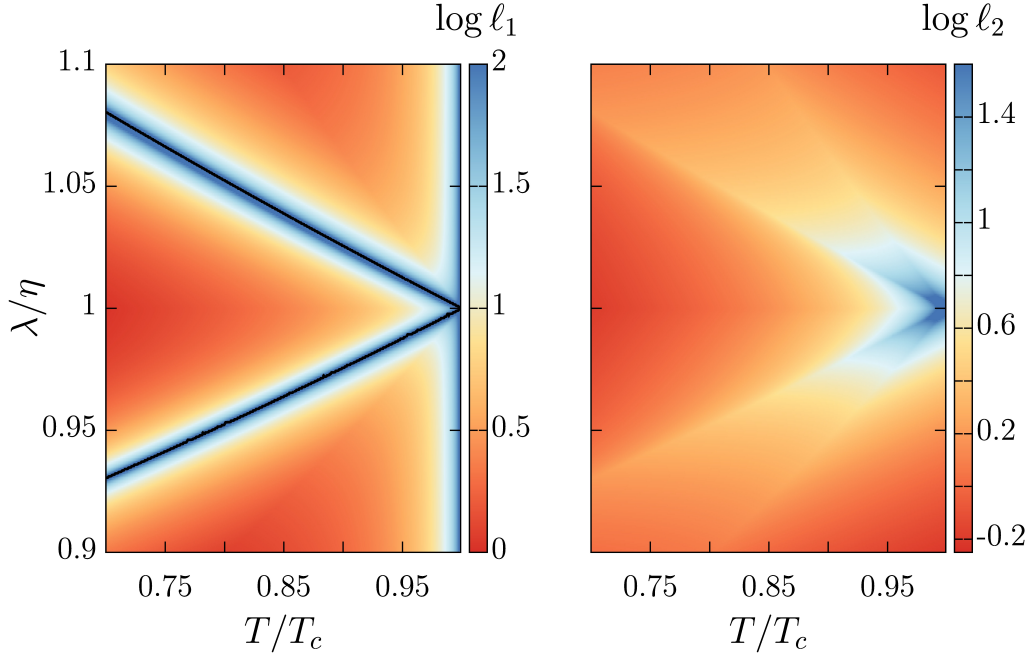


Figure 4. (Color online) – The two largest coherence lengths (smallest eigenvalues of  $\mathcal{M}^2$ ). The left panel shows the largest coherence length  $\ell_1$  that diverges at  $T_c$ , and also when entering the time-reversal symmetry broken ( $s + is$ ) phase. This indicates a second order phase transition denoted by the solid black line. The right panel displays the second largest length scale  $\ell_2$ . Approaching the point where the system breaks  $U(1) \times Z_2$  symmetry, at mean field level, there should be two divergent coherence lengths. Indeed we observe that the second-largest length-scale  $\ell_2$  diverges at a single point at  $T_c$  and where  $\lambda = \eta$ .

$$\mathcal{M}_{f_1 f_1}^2 = \frac{2}{\kappa_1} (\alpha + 3\beta u_1^2 + (\gamma + \delta \cos 2\bar{\varphi})u_2^2 + 3\omega u_1 u_2 \cos \bar{\varphi}) \quad (47a)$$

$$\mathcal{M}_{f_2 f_2}^2 = \frac{2}{\kappa_2} (\alpha + 3\beta u_2^2 + (\gamma + \delta \cos 2\bar{\varphi})u_1^2 + 3\omega u_1 u_2 \cos \bar{\varphi}) \quad (47b)$$

$$\mathcal{M}_{f_1 f_2}^2 = \frac{1}{\sqrt{\kappa_1 \kappa_2}} (4(\gamma + \delta \cos 2\bar{\varphi})u_1 u_2 + (\nu + 3\omega(u_1^2 + u_2^2)) \cos \bar{\varphi}) \quad (47c)$$

$$\mathcal{M}_{\phi\phi}^2 = \frac{\kappa_1 u_1^2 + \kappa_2 u_2^2}{\kappa_1 \kappa_2 u_1^2 u_2^2} (-4\delta u_1^2 u_2^2 \cos 2\bar{\varphi} - (\nu + \omega(u_1^2 + u_2^2))u_1 u_2 \cos \bar{\varphi}) \quad (47d)$$

$$\mathcal{M}_{f_1 \phi}^2 = \sqrt{\frac{\kappa_1 u_1^2 + \kappa_2 u_2^2}{\kappa_1^2 \kappa_2 u_1^2 u_2^2}} (-4\delta u_1 u_2^2 \sin 2\bar{\varphi} - (\nu + \omega(3u_1^2 + u_2^2))u_2 \sin \bar{\varphi}) \quad (47e)$$

$$\mathcal{M}_{f_2 \phi}^2 = \sqrt{\frac{\kappa_1 u_1^2 + \kappa_2 u_2^2}{\kappa_1 \kappa_2^2 u_1^2 u_2^2}} (-4\delta u_1^2 u_2 \sin 2\bar{\varphi} - (\nu + \omega(u_1^2 + 3u_2^2))u_1 \sin \bar{\varphi}) . \quad (47f)$$

Finally, the length scales are given by finding the eigenstates of (46). More precisely, the eigenvalues  $m_i^2$  of the (symmetric) mass matrix  $\mathcal{M}^2$ , whose elements are given in (47), are the (squared) masses of the elementary excitations. The corresponding length scales are the inverse (eigen)masses:  $\ell_i = 1/\sqrt{m_i^2}$ .

The length scales that correspond to the phase diagram Fig. 3 are displayed in Fig. 4 (only the two largest). The largest length scale  $\ell_1$  diverges both at  $T_c$  and at  $T_{Z_2}$ , the temperature of the time-reversal symmetry breaking.

This is the standard mean-field divergence of the coherence length at a two different second order transitions. Notice that the second largest length-scale,  $\ell_2$  diverges at a single point at  $T_c$  and where  $\lambda = \eta$ . This indicates a point of higher symmetry in the phase diagram.

Notice that the other relevant length scale of the theory is the (London) penetration depth  $\lambda_L$  of the magnetic field. It is relatively easy to see that the perturbations of the vector potential completely decouple (at the linear level) from those of the condensates. It is given as the

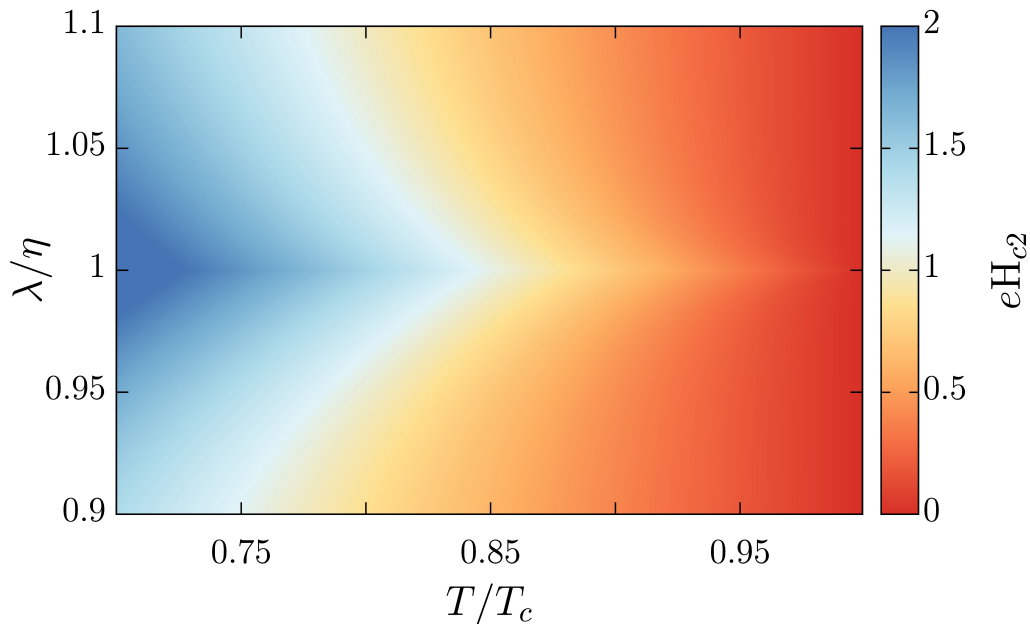


Figure 5. (Color online) – Second critical field calculated from the analysis of the Ginzburg-Landau functional (23) with the coefficients determined consistently from the microscopic theory.

inverse mass of  $\mathbf{A}$  and simply reads as

$$\lambda_L = \frac{1}{e\varrho} = \frac{1}{e\sqrt{\kappa_1|\eta_1|^2 + \kappa_2|\eta_2|^2}}, \quad (48)$$

which can easily be read of Fig. 3. Quite naturally,  $\lambda_L$  is always finite for  $T < T_c$  and diverges when approaching  $T_c$ . So the largest length scale associated with the condensates diverge both at  $T_c$  and at  $T_{\mathbb{Z}_2}$ . It is interesting to note that this automatically imply that  $\lambda_L$  is an intermediate length scale near  $T_{\mathbb{Z}_2}$ . This implies that long-range inter vortex forces are attractive. This is a necessary, though not sufficient condition for non-monotonic interaction between vortices [15, 58].

### C. Second critical field

The perturbation operator (46) can be used not only to determine the relevant length scales of the Ginzburg-Landau theory, but also to obtain the second critical field  $H_{c2}$ . That is by considering the perturbation operator around the normal state. More precisely, in the original parametrization the normal state is  $|\psi_1| = |\psi_2| = 0$ . Using (42), this implies that the normal state in the new variables is  $|\eta_1| = |\eta_2| = 0$  and thus  $u_1 = u_2 = 0$  and  $\bar{\varphi} = 0$ .

Close to the second critical field  $H_{c2}$  the magnetic field is approximately constant:  $\mathbf{B} = B_0 \mathbf{e}_z$  and the densities are small. Thus the Ginzburg-Landau equations (40) can be linearized around the normal state as

$$\Pi^2 \Upsilon = \mathcal{M}^2|_{u_1=u_2=\bar{\varphi}=0} \Upsilon \equiv \mathcal{M}_0^2 \Upsilon. \quad (49)$$

In the Landau Gauge, the vector potential reads as  $\mathbf{A} = (0, B_0 x, 0)^{-1}$ . As a result, the equations read as

$$(\nabla^2 - (eB_0 x)^2) \Upsilon = \mathcal{M}_0^2 \Upsilon. \quad (50)$$

We consider the simple Gaussian ansatz  $\Upsilon = C \exp\left(-\frac{x^2}{2\xi^2}\right)$  with the vector  $C = (C_1, C_2)^T$  and  $eB_0 = 1/\xi^2$ . The equation (50) further simplifies:

$$\mathcal{M}_0^2 \Upsilon = \frac{-1}{\xi^2} \Upsilon. \quad (51)$$

Thus  $1/\xi^2$  is an eigenvalue of  $-\mathcal{M}_0^2$ . More precisely, its largest:

$$eH_{c2} = \frac{1}{\xi^2} := \max\left(\text{Eigenvalue}[-\mathcal{M}_0^2]\right). \quad (52)$$

It is easy to realize from (47) that the perturbations of the relative phase  $\Upsilon$  decouple from density perturbations. The mass matrix thus becomes:

$$\mathcal{M}_0^2 = \begin{pmatrix} 2\alpha/\kappa_1 & \nu/\sqrt{\kappa_1\kappa_2} \\ \nu/\sqrt{\kappa_1\kappa_2} & 2\alpha/\kappa_2 \end{pmatrix}, \quad (53)$$

and its eigenvalues are

$$\frac{\alpha(\kappa_1 + \kappa_2) \pm \sqrt{\alpha^2(\kappa_1 - \kappa_2)^2 - \nu^2\kappa_1\kappa_2}}{\kappa_1\kappa_2}. \quad (54)$$

As a result, we find the second critical field in the dimensionless units of Eq.(23)

$$H_{c2} = \frac{-\alpha(\kappa_1 + \kappa_2) + \sqrt{\alpha^2(\kappa_1 - \kappa_2)^2 - \nu^2\kappa_1\kappa_2}}{e\kappa_1\kappa_2}. \quad (55)$$

Notice that for example that for a given value of  $\kappa_1$ , then having  $\kappa_2 \ll 1$  implies that the second critical field can become very large. Tracing this to the original parametrization implies that if the prefactor of the mixed gradients  $k_{12}$  is close to the critical value  $\sqrt{k_1 k_2}$  where the energy would become unbounded, then the second critical field can become arbitrarily large. This limit for example can be realized for the microscopic coefficients satisfying  $K_1 \gg K_2, K_3$ . Note that the instability never happens since  $\kappa_2$  is always positive. Fig. 5 displays the second critical field as a function of the parameters of the microscopic model.

## V. TOPOLOGICAL EXCITATIONS

The topological properties, as well as the structure of the ground state hints to a rich spectrum of topological excitations, or topological defects, that may occur in the theory of interest. Indeed, the theory features domain-walls that separate between different broken time-reversal phases; vortices that can either carry fractional or integer number of flux quanta. Moreover vortices can further be characterized by  $\mathbb{CP}^1$  invariants and in that case they are referred to as skyrmions. All these topological excitations are potential observable signatures of the  $s + is$  superconducting state.

### A. Domain-walls

The ground state phase which is of principal interest here, is the  $s + is$  superconducting state (32). It is characterized, besides usual spontaneous breakdown of  $U(1)$  gauge symmetry, by a discrete degeneracy due to the relative phase being  $\theta_{12} = \pm\pi/2$ . This discrete degeneracy corresponds to the spontaneous breakdown of the time-reversal symmetry. The spontaneous breakdown of a discrete (here  $\mathbb{Z}_2$ ) symmetry is in general associated with topological excitations in the form of domain walls that interpolate between the two degenerate states. Fig. 6 shows such a domain wall solution interpolating between  $\theta_{12} = -\pi/2$  and  $\theta_{12} = +\pi/2$ .

### B. Flux quantization and vortices

Defining the flux quantization in the original Ginzburg-Landau model (23) requires some careful algebraic calculations because of the mixed gradient terms. This operation becomes elementary in the rewritten Ginzburg-Landau model (37). Indeed the magnetic flux, for exam-

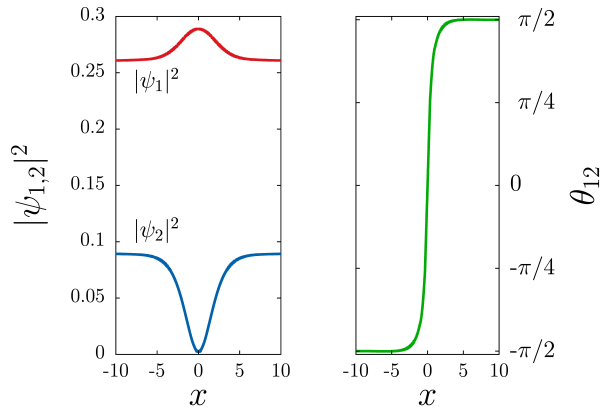


Figure 6. (Color online) – Example of a domain wall that interpolates between two different time-reversal symmetry broken states (i.e.  $\theta_{12} = \pm\pi/2$ ).

ple through the plane, reads as:

$$\Phi = \int_{\mathbb{R}^2} \mathbf{B} \cdot d\mathbf{S} = \oint_{\mathcal{C}} \mathbf{A} \cdot d\boldsymbol{\ell} \quad (56a)$$

$$= \oint_{\mathcal{C}} \frac{\mathbf{J} \cdot d\boldsymbol{\ell}}{e^2 \varrho^2} - \sum_a \frac{\kappa_a |\eta_a|^2}{e \varrho^2} \nabla \varphi_a \cdot d\boldsymbol{\ell} \quad (56b)$$

$$= - \oint_{\mathcal{C}} \sum_a \frac{\kappa_a |\eta_a|^2}{e \varrho^2} \nabla \varphi_a \cdot d\boldsymbol{\ell} \quad (56c)$$

where  $\mathcal{C}$  is the contour of the  $\mathbb{R}^2$  at spatial infinity. To obtain (56a), we use the relation (44) to express the vector potential in terms of the current and phase gradients. Because of the spontaneous breakdown of the  $U(1)$  symmetry, the vector potential is massive and so is the current (Meissner effect). The current should vanish asymptotically (for the energy to be finite) and thus the flux reads as in (56c). The phase of the complex fields  $\varphi_a$  can wind only an integer number of times  $n_a$  and thus  $\oint_{\mathcal{C}} \nabla \varphi_a = 2\pi n_a$ . It follows that if both components have the same winding number  $n_1 = n_2 = n$ , then the flux is quantized:  $\Phi = n\Phi_0$  with the flux quantum  $\Phi_0 = -2\pi/e$ .

There is no formal reason why both  $\eta_{1,2}$  should have the same winding number  $n_{1,2}$ . In that case, the resulting configuration carries only a fraction of the flux quantum. For example consider the simplest case where  $n_1 = 1$  and  $n_2 = 0$ . Then the configuration carries only a fraction  $\kappa_1 |\eta_1|^2 / \varrho^2$  of the flux quantum. Hence it is called a fractional vortex. However, because this gives a nonzero winding of the relative phase in (43) this implies that such a configuration have a logarithmically divergent energy. Indeed, the part of the free energy containing the gradients of the relative phase is  $\int \frac{\kappa_1 \kappa_2 |\eta_1|^2 |\eta_2|^2}{2\varrho^2} (\nabla \varphi_{12})^2$ . At long range, i.e. at a given distance  $r$  for the core, densities are approximately constant and thus its contribution is approximated by

$$\sim \int_{r_0}^r r' dr' \left( \frac{1}{r'} \partial_{\theta} \varphi_{12} \right)^2 \sim \int_{r_0}^r \frac{dr'}{r'} \sim \log \frac{r}{r_0}, \quad (57)$$

This divergence which puts an heavy energy penalty on fractional vortices, is absent if both components have the same winding. As a result, configurations with fractional flux cannot be excited in bulk superconductors. Note however they can be stabilized near boundaries [59], in mesoscopic samples [60–64] or in samples with geometrically trapped domain walls [44]. Note that the condition for flux quantization still allows non-trivial configurations of the magnetic field.

### C. Additional $\mathbb{CP}^1$ invariants – Skyrmions

As discussed in the next subsection, the topological properties of the model can also be understood using the mapping to a nonlinear  $\sigma$ -model. In contrast to the topological invariant characterizing vortices (i.e. the winding number which is defined as a line integral over a closed path), an additional topological  $\mathbb{CP}^1$  index which is in general associated with skyrmionic excitations can be defined [43]. Defining the complex vector  $\boldsymbol{\eta}$  as  $\boldsymbol{\eta}^\dagger = (\sqrt{k_1}\eta_1^*, \sqrt{k_2}\eta_2^*)$ , and provided  $\boldsymbol{\eta} \neq 0$ , the topological  $\mathbb{CP}^1$  index is given as an integral over the  $xy$ -plane :

$$\mathcal{Q}(\boldsymbol{\eta}) = \int_{\mathbb{R}^2} \frac{i\epsilon_{ji}}{2\pi|\boldsymbol{\eta}|^4} \left[ |\boldsymbol{\eta}|^2 \partial_i \boldsymbol{\eta}^\dagger \partial_j \boldsymbol{\eta} + \boldsymbol{\eta}^\dagger \partial_i \boldsymbol{\eta} \partial_j \boldsymbol{\eta}^\dagger \boldsymbol{\eta} \right] dx dy. \quad (58)$$

Provided  $\boldsymbol{\eta} \neq 0$ , the  $\mathbb{CP}^1$  index  $\mathcal{Q}$  is an integer number and is equal to the number of flux quanta:  $\mathcal{Q} = \int B/\Phi_0 = N$  ( $\Phi_0$  being the flux quantum and  $N$  the number of quanta) [43]. As a result, in the case of an axially symmetry vortex with a core where all superconducting condensates simultaneously vanish (i.e.  $\boldsymbol{\eta} = 0$ ), then  $\mathcal{Q} = 0$ . On the other hand, if singularities happen at different locations (i.e.  $\boldsymbol{\eta} \neq 0$ ), then  $\mathcal{Q} \neq 0$  and the quantization condition holds. As a result,  $\mathcal{Q}$  is a useful quantity that can discriminate between vortices and skyrmions. See Ref. [43] for a rigorous discussion. One should note that the flux-quantization condition (56) and the integral formula for the topological charge  $\mathcal{Q}$  above are valid only for field configurations for which  $\boldsymbol{\eta}$  never vanishes. Note that flux is also quantized for ordinary vortices, for which  $\boldsymbol{\eta}$  vanishes, but then it is no longer associated with the the topological charge  $\mathcal{Q}$ , but with a  $U(1)$  topological invariant (the usual winding number).

### D. Mapping to a nonlinear $\sigma$ -model

The mapping to the nonlinear  $\sigma$ -model consists of rewriting the theory in term a massive  $U(1)$  vector field (the current) coupled to a compact  $O(3)$  vector. Importantly in this kind of mapping the supercurrent is coupled to Faddeev-Skyrme terms [65]. Starting from the theory in terms of charged and neutral modes (43), it is possible to map the two-component model to an easy-plane non-linear  $\sigma$ -model. This mapping is done by defining the

pseudo-spin unit vector  $\mathbf{n}$  as a projection of the superconducting degrees of freedom onto spin-1/2 Pauli matrices  $\boldsymbol{\sigma}$ :

$$\mathbf{n} = \frac{\boldsymbol{\eta}^\dagger \boldsymbol{\sigma} \boldsymbol{\eta}}{\boldsymbol{\eta}^\dagger \boldsymbol{\eta}}, \quad \text{where } \boldsymbol{\eta}^\dagger = (\sqrt{k_1}\eta_1^*, \sqrt{k_2}\eta_2^*). \quad (59)$$

The following identity is useful to rewrite the free energy (43) in terms of the pseudo-spin  $\mathbf{n}$ , total density  $\varrho^2 := \boldsymbol{\eta}^\dagger \boldsymbol{\eta}$  and gauge invariant current  $\mathbf{J}$

$$\frac{\varrho^2}{4} \partial_k n_a \partial_k n_a + (\nabla \varrho)^2 = \frac{\kappa_1 \kappa_2 |\eta_1|^2 |\eta_2|^2}{\varrho^2} (\nabla \varphi_{12})^2 + \sum_a \kappa_a (\nabla |\eta_a|)^2, \quad (60)$$

where summation on repeated indices is implied. Using the definition of the current and noting that

$$4\epsilon_{ijk} \partial_i \left( \sum_a \frac{\kappa_a |\eta_a|^2}{\varrho^2} \partial_j \varphi_a \right) = \epsilon_{ijk} \epsilon_{abc} n_a \partial_i n_b \partial_j n_c, \quad (61)$$

where  $\epsilon$  is the Levi-Civita symbol, the magnetic field reads

$$B_k = \frac{1}{e} \epsilon_{ijk} \left( \partial_i \left( \frac{J_j}{e\varrho^2} \right) - \frac{1}{4} \epsilon_{abc} n_a \partial_i n_b \partial_j n_c \right), \quad (62)$$

and the free energy (43) can be written as

$$\mathcal{F} = \frac{1}{2} (\nabla \varrho)^2 + \frac{\varrho^2}{8} \partial_k n_a \partial_k n_a + \frac{\mathbf{J}^2}{2e^2 \varrho^2} + V(\varrho, \mathbf{n}) + \frac{1}{2e^2} \left[ \epsilon_{ijk} \left( \partial_i \left( \frac{J_j}{e\varrho^2} \right) - \frac{1}{4} \epsilon_{abc} n_a \partial_i n_b \partial_j n_c \right) \right]^2, \quad (63)$$

where  $V(\varrho, \mathbf{n})$  is the potential terms

$$V = \frac{\varrho^2}{2} (a_1 + a_2 n_x) + \frac{\varrho^4}{4} (b_1 + 2b_2 n_x + b_3 n_x^2 + b_4 n_z^2), \quad (64)$$

with the coefficients

$$b_1 = \beta + \gamma - 4\delta, \quad b_2 = 2\omega, \quad b_3 = 8\delta, \quad b_4 = \beta - \gamma + 4\delta, \\ a_1 = 2\alpha, \quad a_2 = 2\nu. \quad (65)$$

The pseudo-spin is a map from the one-point compactification of the plane ( $\mathbb{R}^2 \simeq S^2$ ) to the two-sphere target space spanned by  $\mathbf{n}$ . That is  $\mathbf{n} : S^2 \rightarrow S^2$ , classified by the homotopy class  $\pi_2(S^2) \in \mathbb{Z}$ , thus defining the integer valued topological (skyrmionic) charge

$$\mathcal{Q}(\mathbf{n}) = \frac{1}{4\pi} \int_{\mathbb{R}^2} \mathbf{n} \cdot \partial_x \mathbf{n} \times \partial_y \mathbf{n} \, dx dy. \quad (66)$$

Heuristically, the topological charge (66) can be understood as the integer that counts the number of times the pseudo-spin wraps the target sphere. If a field configuration spans only a portion of the target sphere, then the associated flux needs not to be quantized.

## VI. CONCLUSION

To summarize, we presented a microscopic derivation for  $N$ -component Ginzburg-Landau models with a focus on the time-reversal-symmetry-breaking  $s + is$  state for a three-band microscopic model. This model is widely believed to describe hole-doped 122 compounds. We consistently derived the two-component Ginzburg-Landau functional that is relevant for the case of an interband-dominated pairing. We discussed the elementary prop-

erties of these models: normal modes and length-scales, critical fields and basic topological defects.

## ACKNOWLEDGMENTS

The work was supported by the Swedish Research Council Grants No. 642-2013-7837. The computations were performed on resources provided by the Swedish National Infrastructure for Computing (SNIC) at National Supercomputer Center at Linköping, Sweden.

- 
- [1] I.I. Mazin and V.P. Antropov, “Electronic structure, electron-phonon coupling, and multiband effects in  $\text{MgB}_2$ ,” *Physica C: Superconductivity* **385**, 49 – 65 (2003).
  - [2] A. Damascelli, D. H. Lu, K. M. Shen, N. P. Armitage, F. Ronning, D. L. Feng, C. Kim, Z.-X. Shen, T. Kimura, Y. Tokura, Z. Q. Mao, and Y. Maeno, “Fermi Surface, Surface States, and Surface Reconstruction in  $\text{Sr}_2\text{RuO}_4$ ,” *Phys. Rev. Lett.* **85**, 5194–5197 (2000).
  - [3] Yoichi Kamihara, Takumi Watanabe, Masahiro Hirano, and Hideo Hosono, “Iron-Based Layered Superconductor  $\text{La}[\text{O}_{1-x}\text{F}_x]\text{FeAs}$  ( $x = 0.05\text{--}0.12$ ) with  $T_c = 26\text{ K}$ ,” *Journal of the American Chemical Society* **130**, 3296–3297 (2008).
  - [4] I. I. Mazin, D. J. Singh, M. D. Johannes, and M. H. Du, “Unconventional Superconductivity with a Sign Reversal in the Order Parameter of  $\text{LaFeAsO}_{1-x}\text{F}_x$ ,” *Phys. Rev. Lett.* **101**, 057003 (2008).
  - [5] Kazuhiko Kuroki, Seiichiro Onari, Ryotaro Arita, Hidetomo Usui, Yukio Tanaka, Hiroshi Kontani, and Hideo Aoki, “Unconventional Pairing Originating from the Disconnected Fermi Surfaces of Superconducting  $\text{LaFeAsO}_{1-x}\text{F}_x$ ,” *Phys. Rev. Lett.* **101**, 087004 (2008).
  - [6] A. V. Chubukov, D. V. Efremov, and I. Eremin, “Magnetism, superconductivity, and pairing symmetry in iron-based superconductors,” *Phys. Rev. B* **78**, 134512 (2008).
  - [7] A.V. Balatsky, “Field-induced  $d_{x^2-y^2} + id_{xy}$  state and marginal stability of high- $T_c$  superconductor,” *Physica C: Superconductivity* **332**, 337 – 342 (2000).
  - [8] Wei-Cheng Lee, Shou-Cheng Zhang, and Congjun Wu, “Pairing State with a Time-Reversal Symmetry Breaking in FeAs-Based Superconductors,” *Phys. Rev. Lett.* **102**, 217002 (2009).
  - [9] Christian Platt, Ronny Thomale, Carsten Honerkamp, Shou-Cheng Zhang, and Werner Hanke, “Mechanism for a pairing state with time-reversal symmetry breaking in iron-based superconductors,” *Phys. Rev. B* **85**, 180502 (2012).
  - [10] Valentin Stanev and Zlatko Tešanović, “Three-band superconductivity and the order parameter that breaks time-reversal symmetry,” *Phys. Rev. B* **81**, 134522 (2010).
  - [11] Rafael M. Fernandes and Andrew J. Millis, “Nematicity as a Probe of Superconducting Pairing in Iron-Based Superconductors,” *Phys. Rev. Lett.* **111**, 127001 (2013).
  - [12] D. F. Agterberg, Victor Barzykin, and Lev P. Gor’kov, “Conventional mechanisms for exotic superconductivity,” *Phys. Rev. B* **60**, 14868–14871 (1999).
  - [13] T. K. Ng and N. Nagaosa, “Broken time-reversal symmetry in Josephson junction involving two-band superconductors,” *Europhysics Letters* **87**, 17003–+ (2009).
  - [14] Shi-Zeng Lin and Xiao Hu, “Massless Leggett Mode in Three-Band Superconductors with Time-Reversal-Symmetry Breaking,” *Phys. Rev. Lett.* **108**, 177005 (2012).
  - [15] Johan Carlström, Julien Garaud, and Egor Babaev, “Length scales, collective modes, and type-1.5 regimes in three-band superconductors,” *Phys. Rev. B* **84**, 134518 (2011).
  - [16] A. M. Bobkov and I. V. Bobkova, “Time-reversal symmetry breaking state near the surface of an  $s_{\pm}$  superconductor,” *Phys. Rev. B* **84**, 134527 (2011).
  - [17] Saurabh Maiti and Andrey V. Chubukov, “ $s + is$  state with broken time-reversal symmetry in Fe-based superconductors,” *Phys. Rev. B* **87**, 144511 (2013).
  - [18] Saurabh Maiti, Manfred Sigrist, and Andrey Chubukov, “Spontaneous currents in a superconductor with  $s + is$  symmetry,” *Phys. Rev. B* **91**, 161102 (2015).
  - [19] H. Ding, P. Richard, K. Nakayama, K. Sugawara, T. Arakane, Y. Sekiba, A. Takayama, S. Souma, T. Sato, T. Takahashi, Z. Wang, X. Dai, Z. Fang, G. F. Chen, J. L. Luo, and N. L. Wang, “Observation of Fermi-surface-dependent nodeless superconducting gaps in  $\text{Ba}_{0.6}\text{K}_{0.4}\text{Fe}_2\text{As}_2$ ,” *EPL (Europhysics Letters)* **83**, 47001 (2008).
  - [20] R. Khasanov, D. V. Evtushinsky, A. Amato, H.-H. Klauss, H. Luetkens, Ch. Niedermayer, B. Büchner, G. L. Sun, C. T. Lin, J. T. Park, D. S. Inosov, and V. Hinkov, “Two-Gap Superconductivity in  $\text{Ba}_{1-x}\text{K}_x\text{Fe}_2\text{As}_2$ : A Complementary Study of the Magnetic Penetration Depth by Muon-Spin Rotation and Angle-Resolved Photoemission,” *Phys. Rev. Lett.* **102**, 187005 (2009).
  - [21] K. Nakayama, T. Sato, P. Richard, Y.-M. Xu, T. Kawahara, K. Umezawa, T. Qian, M. Neupane, G. F. Chen, H. Ding, and T. Takahashi, “Universality of superconducting gaps in overdoped  $\text{Ba}_{0.3}\text{K}_{0.7}\text{Fe}_2\text{As}_2$  observed by angle-resolved photoemission spectroscopy,” *Phys. Rev. B* **83**, 020501 (2011).
  - [22] X. G. Luo, M. A. Tanatar, J.-Ph. Reid, H. Shakeripour, N. Doiron-Leyraud, N. Ni, S. L. Bud’ko, P. C. Canfield, Huiqian Luo, Zhaosheng Wang, Hai-Hu Wen, R. Prozorov, and Louis Taillefer, “Quasiparticle heat transport in single-crystalline  $\text{Ba}_{1-x}\text{K}_x\text{Fe}_2\text{As}_2$ : Evidence for a  $k$ -dependent superconducting gap without nodes,” *Phys.*



- Rev. B **80**, 140503 (2009).
- [23] A. D. Christianson, E. A. Goremychkin, R. Osborn, S. Rosenkranz, M. D. Lumsden, C. D. Malliakas, I. S. Todorov, H. Claus, D. Y. Chung, M. G. Kanatzidis, R. I. Bewley, and T. Guidi, “Unconventional superconductivity in  $\text{Ba}_{0.6}\text{K}_{0.4}\text{Fe}_2\text{As}_2$  from inelastic neutron scattering,” *Nature* **456**, 930–932 (2008).
  - [24] S. Maiti, M. M. Korshunov, T. A. Maier, P. J. Hirschfeld, and A. V. Chubukov, “Evolution of the Superconducting State of Fe-Based Compounds with Doping,” *Phys. Rev. Lett.* **107**, 147002 (2011).
  - [25] S. Maiti, M. M. Korshunov, T. A. Maier, P. J. Hirschfeld, and A. V. Chubukov, “Evolution of symmetry and structure of the gap in iron-based superconductors with doping and interactions,” *Phys. Rev. B* **84**, 224505 (2011).
  - [26] J-Ph Reid, A Juneau-Fecteau, R T Gordon, S René de Cotret, N Doiron-Leyraud, X G Luo, H Shakeripour, J Chang, M A Tanatar, H Kim, R Prozorov, T Saito, H Fukazawa, Y Kohori, K Kihou, C H Lee, A Iyo, H Eisaki, B Shen, H-H Wen, and Louis Taillefer, “From d-wave to s-wave pairing in the iron-pnictide superconductor  $(\text{Ba,K})\text{Fe}_2\text{As}_2$ ,” *Superconductor Science and Technology* **25**, 084013 (2012).
  - [27] J.-Ph. Reid, M. A. Tanatar, A. Juneau-Fecteau, R. T. Gordon, S. René de Cotret, N. Doiron-Leyraud, T. Saito, H. Fukazawa, Y. Kohori, K. Kihou, C. H. Lee, A. Iyo, H. Eisaki, R. Prozorov, and Louis Taillefer, “Universal Heat Conduction in the Iron Arsenide Superconductor  $\text{KFe}_2\text{As}_2$ : Evidence of a *d*-Wave State,” *Phys. Rev. Lett.* **109**, 087001 (2012).
  - [28] F. F. Tafti, A. Juneau-Fecteau, M-E. Delage, S. Rene de Cotret, J-Ph. Reid, A. F. Wang, X-G. Luo, X. H. Chen, N. Doiron-Leyraud, and Louis Taillefer, “Sudden reversal in the pressure dependence of  $T_c$  in the iron-based superconductor  $\text{KFe}_2\text{As}_2$ ,” *Nature Physics* **9**, 349–352 (2013).
  - [29] F. F. Tafti, J. P. Clancy, M. Lapointe-Major, C. Collignon, S. Faucher, J. A. Sears, A. Juneau-Fecteau, N. Doiron-Leyraud, A. F. Wang, X.-G. Luo, X. H. Chen, S. Desgreniers, Young-June Kim, and Louis Taillefer, “Sudden reversal in the pressure dependence of  $T_c$  in the iron-based superconductor  $\text{CsFe}_2\text{As}_2$ : A possible link between inelastic scattering and pairing symmetry,” *Phys. Rev. B* **89**, 134502 (2014).
  - [30] D. Watanabe, T. Yamashita, Y. Kawamoto, S. Kurata, Y. Mizukami, T. Ohta, S. Kasahara, M. Yamashita, T. Saito, H. Fukazawa, Y. Kohori, S. Ishida, K. Kihou, C. H. Lee, A. Iyo, H. Eisaki, A. B. Vorontsov, T. Shibauchi, and Y. Matsuda, “Doping evolution of the quasiparticle excitations in heavily hole-doped  $\text{Ba}_{1-x}\text{K}_x\text{Fe}_2\text{As}_2$ : A possible superconducting gap with sign-reversal between hole pockets,” *Phys. Rev. B* **89**, 115112 (2014).
  - [31] K. Okazaki, Y. Ota, Y. Kotani, W. Malaeb, Y. Ishida, T. Shimojima, T. Kiss, S. Watanabe, C.-T. Chen, K. Kihou, C. H. Lee, A. Iyo, H. Eisaki, T. Saito, H. Fukazawa, Y. Kohori, K. Hashimoto, T. Shibauchi, Y. Matsuda, H. Ikeda, H. Miyahara, R. Arita, A. Chainani, and S. Shin, “Octet-Line Node Structure of Superconducting Order Parameter in  $\text{KFe}_2\text{As}_2$ ,” *Science* **337**, 1314–1317 (2012).
  - [32] Robert Joynt, “Upward curvature of  $H_{c2}$  in high- $T_c$  superconductors: Possible evidence for *s* - *d* pairing,” *Phys. Rev. B* **41**, 4271–4277 (1990).
  - [33] Q. P. Li, B. E. C. Koltenbah, and Robert Joynt, “Mixed *s*-wave and *d*-wave superconductivity in high- $T_c$  systems,” *Phys. Rev. B* **48**, 437–455 (1993).
  - [34] A. J. Berlinsky, A. L. Fetter, M. Franz, C. Kallin, and P. I. Soininen, “Ginzburg-Landau Theory of Vortices in *d*-Wave Superconductors,” *Phys. Rev. Lett.* **75**, 2200–2203 (1995).
  - [35] Ronny Thomale, Christian Platt, Werner Hanke, Jiangping Hu, and B. A. Bernevig, “Exotic *d*-Wave Superconducting State of Strongly Hole-Doped  $\text{K}_x\text{Ba}_{1-x}\text{Fe}_2\text{As}_2$ ,” *Phys. Rev. Lett.* **107**, 117001 (2011).
  - [36] Katsuhiko Suzuki, Hidetomo Usui, and Kazuhiko Kuroki, “Spin fluctuations and unconventional pairing in  $\text{KFe}_2\text{As}_2$ ,” *Phys. Rev. B* **84**, 144514 (2011).
  - [37] S. Maiti, M. M. Korshunov, and A. V. Chubukov, “Gap symmetry in  $\text{KFe}_2\text{As}_2$  and the  $\cos 4\theta$  gap component in  $\text{LiFeAs}$ ,” *Phys. Rev. B* **85**, 014511 (2012).
  - [38] F. Ahn, I. Eremin, J. Knolle, V. B. Zabolotnyy, S. V. Borisenko, B. Büchner, and A. V. Chubukov, “Superconductivity from repulsion in  $\text{LiFeAs}$ : Novel *s*-wave symmetry and potential time-reversal symmetry breaking,” *Phys. Rev. B* **89**, 144513 (2014).
  - [39] Andrew Peter Mackenzie and Yoshiteru Maeno, “The superconductivity of  $\text{Sr}_2\text{RuO}_4$  and the physics of spin-triplet pairing,” *Rev. Mod. Phys.* **75**, 657–712 (2003).
  - [40] Valentin Stanev, “Model of collective modes in three-band superconductors with repulsive interband interactions,” *Phys. Rev. B* **85**, 174520 (2012).
  - [41] M. Mariani, L. Fanfarillo, C. Castellani, and L. Benfatto, “Leggett modes in iron-based superconductors as a probe of time-reversal symmetry breaking,” *Phys. Rev. B* **88**, 214508 (2013).
  - [42] Julien Garaud, Johan Carlström, and Egor Babaev, “Topological Solitons in Three-Band Superconductors with Broken Time Reversal Symmetry,” *Phys. Rev. Lett.* **107**, 197001 (2011).
  - [43] Julien Garaud, Johan Carlström, Egor Babaev, and Martin Speight, “Chiral  $CP^2$  skyrmions in three-band superconductors,” *Phys. Rev. B* **87**, 014507 (2013).
  - [44] Julien Garaud and Egor Babaev, “Domain Walls and Their Experimental Signatures in *s* + *is* Superconductors,” *Phys. Rev. Lett.* **112**, 017003 (2014).
  - [45] Mihail Silaev and Egor Babaev, “Unusual mechanism of vortex viscosity generated by mixed normal modes in superconductors with broken time reversal symmetry,” *Phys. Rev. B* **88**, 220504 (2013).
  - [46] Troels Arnfred Bojesen, Egor Babaev, and Asle Sudbø, “Time reversal symmetry breakdown in normal and superconducting states in frustrated three-band systems,” *Phys. Rev. B* **88**, 220511 (2013).
  - [47] Troels Arnfred Bojesen, Egor Babaev, and Asle Sudbø, “Phase transitions and anomalous normal state in superconductors with broken time-reversal symmetry,” *Phys. Rev. B* **89**, 104509 (2014).
  - [48] Johan Carlström and Egor Babaev, “Spontaneous breakdown of time-reversal symmetry induced by thermal fluctuations,” *Phys. Rev. B* **91**, 140504 (2015).
  - [49] Alberto Hinojosa, Rafael M. Fernandes, and Andrey V. Chubukov, “Time-Reversal Symmetry Breaking Superconductivity in the Coexistence Phase with Magnetism in Fe Pnictides,” *Phys. Rev. Lett.* **113**, 167001 (2014).
  - [50] Mihail Silaev, Julien Garaud, and Egor Babaev, “Unconventional thermoelectric effect in superconductors that break time-reversal symmetry,” *Phys. Rev. B* **92**, 174510 (2015).

- (2015).
- [51] J. Garaud, M. Silaev, and E. Babaev, “Thermoelectric signatures of time-reversal symmetry breaking states in multiband superconductors,” (2015), [arXiv:1507.04712 \[cond-mat.supr-con\]](#).
  - [52] A. B. Vorontsov, I. Vekhter, and M. Eschrig, “Surface Bound States and Spin Currents in Noncentrosymmetric Superconductors,” *Phys. Rev. Lett.* **101**, 127003 (2008).
  - [53] Mihail Silaev and Egor Babaev, “Microscopic derivation of two-component Ginzburg-Landau model and conditions of its applicability in two-band systems,” *Phys. Rev. B* **85**, 134514 (2012).
  - [54] D R Tilley, “The Ginzburg-Landau equations for pure two band superconductors,” *Proceedings of the Physical Society* **84**, 573 (1964).
  - [55] A. Gurevich, “Enhancement of the upper critical field by nonmagnetic impurities in dirty two-gap superconductors,” *Phys. Rev. B* **67**, 184515 (2003).
  - [56] M. E. Zhitomirsky and V.-H. Dao, “Ginzburg-Landau theory of vortices in a multigap superconductor,” *Phys. Rev. B* **69**, 054508 (2004).
  - [57] A. Gurevich, “Limits of the upper critical field in dirty two-gap superconductors,” *Physica C: Superconductivity* **456**, 160 – 169 (2007), recent Advances in MgB2 Research.
  - [58] Johan Carlström, Egor Babaev, and Martin Speight, “Type-1.5 superconductivity in multiband systems: Effects of interband couplings,” *Phys. Rev. B* **83**, 174509 (2011).
  - [59] M. A. Silaev, “Stable fractional flux vortices and unconventional magnetic state in two-component superconductors,” *Phys. Rev. B* **83**, 144519 (2011).
  - [60] Egor Babaev, “Vortices carrying an arbitrary fraction of magnetic flux quantum in two-gap superconductors,” *Phys. Rev. Lett.* **89**, 067001 (2002).
  - [61] Hendrik Bluhm, Nicholas C. Koshnick, Martin E. Huber, and Kathryn A. Moler, “Magnetic Response of Mesoscopic Superconducting Rings with Two Order Parameters,” *Phys. Rev. Lett.* **97**, 237002 (2006).
  - [62] L. F. Chibotaru, V. H. Dao, and A. Ceulemans, “Thermodynamically stable noncomposite vortices in mesoscopic two-gap superconductors,” *EPL (Europhysics Letters)* **78**, 47001 (2007).
  - [63] L. F. Chibotaru and V. H. Dao, “Stable fractional flux vortices in mesoscopic superconductors,” *Phys. Rev. B* **81**, 020502 (2010).
  - [64] R. Geurts, M. V. Milošević, and F. M. Peeters, “Vortex matter in mesoscopic two-gap superconducting disks: Influence of Josephson and magnetic coupling,” *Phys. Rev. B* **81**, 214514 (2010).
  - [65] Egor Babaev, L. D. Faddeev, and Antti J. Niemi, “Hidden symmetry and knot solitons in a charged two-condensate Bose system,” *Phys. Rev. B* **65**, 100512 (2002).